

Application of Large-Eddy Simulations in Evaluating Ventilation over 3D Building Data Retrieved from Satellite Images

Weiwen Wang¹, Yong Xu², and Edward Ng³

¹ School of Architecture, The Chinese University of Hong Kong
Shatin, N.T., Hong Kong SAR, China
e-mail: w.wang@cuhk.edu.hk

² Institute of Future Cities, The Chinese University of Hong Kong
Shatin, N.T., Hong Kong SAR, China
e-mail: xuyong@cuhk.edu.hk

³ School of Architecture, Institute of Environment, Energy, and Sustainability, and Institute of Future Cities, The Chinese University of Hong Kong
Shatin, N.T., Hong Kong SAR, China
e-mail: edwardng@cuhk.edu.hk

Keywords: Large-Eddy Simulation, Urban Ventilation, Building Height Extraction.

Abstract. *Computational fluid dynamics (CFD) techniques, such as the Reynolds-averaged Navier-Stokes (RANS) model and large-eddy simulations (LES), are widely used in urban ventilation studies. Unfortunately, realistic digital elevations of urban areas required in CFD studies are not always available. Therefore, there is a need to extract urban information from satellite images that can be used for, but not limited to, studies of the urban wind environment. This study evaluates 3D building geometries extracted from different satellite images by LES of pedestrian-level ventilation. As a case study, three sets of digital elevation data extracted from satellite images in an urban area of Mong Kok, Hong Kong, are assessed. The LES model, entitled the Parallelized LES Model (PALM), is first validated by a CFD guideline of simulating flows around single building. Wind characteristics in urban elevations extracted from two single satellite images and the fused result are then compared with those from realistic data in the same area, using identical LES settings. The result shows that building heights extracted from the TerraSAR-X synthetic aperture radar (SAR) image and the fused results of SAR and the WorldView-2 optical (Stereo) images are reasonable for air ventilation assessment (AVA). Better performance in representing tall buildings, rather than low buildings, is found to be more important in building height extraction for AVA purposes.*

1. Introduction

According to the World Health Organization (WHO), the urban population in 2014 accounted for 54% of the total global population, up from 34% in 1960, and it continues to grow. Rapid urbanization causes a number of problems such as urban heat islands (UHIs) and air pollution, which threaten the health of city inhabitants. Urban ventilation is found to be a way of mitigating these problems [Arnfield, 2003; Ng, 2009; Shi, 2015; Wong, 2011]. Good air ventilation is very important for high-quality and healthy living, particularly for high-density cities in tropical and subtropical regions with a hot and humid climate. Thermal comfort can be achieved by capturing natural wind. To achieve neutral thermal sensation in an urban environment, a wind speed of 0.9–1.3 m/s is needed for a person wearing light clothing under shaded conditions [Ng, 2012].

In the literature of urban air ventilation studies, various research methods have been used to describe the complex flows over urban environments. Computational fluid dynamics (CFD) techniques such as the Reynolds-averaged Navier-Stokes (RANS) model, large-eddy simulation (LES), and direct numerical simulation (DNS) are among the commonly used tools [Brunner, 2003; Ng, 2011]. Urban ventilation is strongly influenced by wind speed and direction, which in turn are affected by three-dimensional urban morphology [Ramponi, 2015; Skote, 2005; Yang, 2013]. Unfortunately, realistic digital elevations of urban areas required in CFD studies are not always available for open access, especially in the less developed regions of the world where urban population growth is concentrated. Furthermore, surface geometries and urban morphologies are found to have a significant influence on UHI [Unger, 2004], especially for regions with a hot and humid microclimate [Emmanuel, 2006]. High-resolution digital elevations have been extensively used in studies of urban climate and outdoor thermal comfort [Lindberg, 2010]. Therefore, there is a need to develop methodologies of extracting building heights in urban areas from satellite images that can be used for, but not limited to, studies of urban ventilation.

There are three kinds of building height extraction from available remote sensing data: Stereo photogrammetry technology with pairs of optical images (hereafter referred to as Stereo images), synthetic aperture radar (SAR) technology, and light detection and ranging data (LiDAR) technology. However, there are limitations to these methods: (1) Stereo images tend to underestimate the height of tall buildings, and taller buildings predict larger errors [Eckert, 2010]; (2) the interferometry of SAR provides noisy and incomplete data, particularly for high-density urban areas where mutual interference of surrounding buildings are significant [Colin-Koeniguer, 2014; Sportouche, 2011]; and (3) LiDAR data is expensive and is limited by flight restrictions for applications in large urban areas [Zhou, 2014]. Therefore, recent studies have also been devoted to the integrated use of different kinds of data for building height retrieval [Sportouche, 2011; Xu, 2015; Zhou, 2014].

The objective of the present study is to assess the performance of building height extractions from different kinds of satellite images for potential use in urban ventilation studies with CFD techniques. Evaluation of building height extraction from satellite images from the perspective of a particular application, i.e., urban ventilation, has rarely been attempted to date as far as we know. What affects pedestrian comfort directly is the wind flow

within cities, in particular, the local turbulence level [Britter, 2003]. We therefore use an LES model to produce CFD simulations in this study. LES overcomes the deficiencies of RANS by explicitly resolving large, energy-containing turbulent eddies and parameterizing only small (subgrid) scale turbulence [Rodi, 1997; Tamura, 2008]. The dimensionality, spatial resolution, and turbulence intensity that an LES model can handle are superior compared to most of the other methodologies, and sometimes also to other CFD models, i.e., RANS and DNS [Castillo, 2011]. LES provides not only mean flow fields but also instantaneous turbulences, which are especially important for human comfort at the pedestrian level in the urban canopy layer [Keck, 2014].

2 Neighborhood-Scale Urban Geometries

An approach that jointly uses high-resolution WorldView-2 Stereo images and multi-temporal TerraSAR-X SAR images to retrieve building heights in high-density urban areas, which has the advantage of both datasets, was proposed by a recent study in Hong Kong [Xu, 2015]. In the present study, actual (measured) urban elevations (building heights) in a neighborhood on the Kowloon Peninsula provided by the Hong Kong Planning Department are utilized as topography input for the LES model. It is the same domain of Mong Kok used in Xu [2015], given in Figure 1a. Both are $1.2\text{km} \times 1.2\text{ km}$ and have a horizontal resolution of 2m. The methodology proposed by Xu [2015] for retrieving building heights in urban areas using both Stereo and SAR images assumes that the building footprints are known and involves two main stages: First, estimated initial building heights are retrieved from Stereo and SAR images, respectively; second, according to an object-based fusion approach, the initial building heights are then combined. The bias of building heights between actual data and data extracted from Stereo images, SAR images, and the fused result of the two kinds of images is given in Figure 1b, c, and d, respectively.

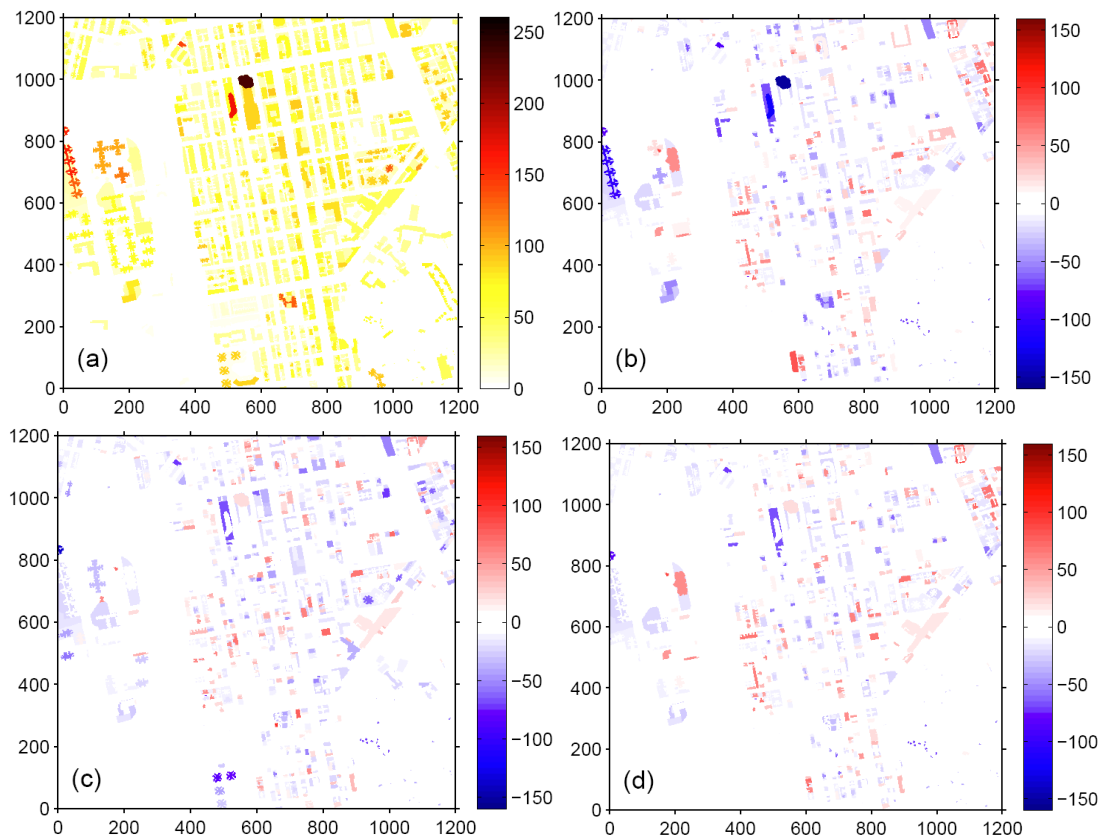


Figure 1: (a) Actual urban elevations (building heights) in a $1.2\text{km} \times 1.2\text{km}$ neighborhood in Mong Kok. Bias between actual data and data extracted from (b) Stereo images, (c) SAR images, and (d) fused result of the two kinds of images

3 The Parallelized Large-Eddy Simulation Model (PALM)

The LES model used in this study is the Parallelized LES Model (PALM) for atmospheric and oceanic flows, which has been developed at the Institute of Meteorology and Climatology of the Leibniz Universität Hannover since 1997 [Raasch, 2001]. PALM has been validated for simulating flows and turbulence characteristics at the street-canyon and neighbourhood scale [Letzel, 2008] and has been widely used in studies of urban street-canyon flows in recent years [Inagaki, 2011; Kanda, 2013; Park, 2014; Park, 2012; Razak, 2013], including high-density urban areas in Hong Kong [Letzel, 2012] and Macau [Keck, 2014]. The code used in this study is the most updated PALM version 4.0 [Maronga, 2015]. More details can be found on the PALM homepage (<https://palm.muk.uni-hannover.de/trac>).

3.1 Indicator and simulation setup

In air ventilation assessment (AVA) studies, we are especially interested in the pedestrian-level wind velocity. The wind velocity ratio (VR) is used as an indicator, which is calculated by

$$VR = V_p / V_\infty \quad (1)$$

where V_p is the wind velocity at the pedestrian level (2m above the ground), and V_∞ is the wind velocity at the top of the wind boundary layer and is not affected by ground roughness [Ng, 2009]. A top boundary layer of 500m is commonly used in Hong Kong AVA studies [Hong Kong Planning Department, 2008].

As we are focusing mainly on VR, the input wind speed is not very important, and if high wind speed is used, more computational time will be needed because the time step has to be shorter. Therefore, a low-velocity geostrophic wind of 1.5 m/s [Keck, 2014] is prescribed to save computational time. The time step sizes are optimized in PALM. Horizontal grid sizes are equidistantly 2m. The vertical grid spacing is 2m below 300m and stretched with a stretch factor of 1.08 above. CFD equations are spatially discretized on an Arakawa-C grid in PALM. Scalar variables are defined at the grid centers, while velocity components are shifted by half of the grid spacing. Therefore, horizontal wind velocity output from the 1m and 3m levels is linearly interpolated (averaged) to obtain V_p at 2m above the ground. V_∞ is derived from 500m. The total simulation time is 6 hours. The first 4 hours are excluded in the analysis of the results, as the turbulences need this time to spin-up. The simulated results from the 5th to the 6th hours are averaged for analysis. East and southwest (225°) winds, the prevailing annual and summer winds in Hong Kong, respectively, are simulated for assessment of building height extraction from satellite images. The no-slip bottom boundary condition with a Prandtl layer and the free-slip top boundary condition are applied to horizontal velocity components. As the targeted area is surrounded by urban areas, a simple cyclic (periodic) boundary condition setup in both the streamwise and spanwise directions is sufficient for the task. The simulations are restricted to neutral atmospheric stratification, i.e., thermal effects are not considered.

By default, PALM has six prognostic quantities. But as neutral stratification assumption is adopted, calculation of temperature equation is switched off. Variables including the velocity components u , v , w and the subgrid-scale turbulent kinetic energy e will be involved in our calculations, while the potential temperature θ , specific humidity q_v or a passive scalar s will not be involved. The separation of resolved scales and subgrid-scales is implicitly achieved by averaging the governing equations over discrete Cartesian grid volumes [Maronga, 2015]. Time step lengths are optimized by PALM codes and varying. For our main runs, the

maximum value of time step is 20 seconds, and the number of time steps for a simulation time of 21,600 seconds are around 20,000~25,000.

3.2 Model validation

We use the CFD guidelines proposed by a working group from the Architectural Institute of Japan (AIJ) to verify the PALM codes. To calibrate CFD simulations of air ventilation, AIJ guidelines conducted a series of cross-comparisons of wind data from RANS, LES, DNS, and wind tunnel tests [Tominaga, 2008]. We conducted a LES experiment of the 2:1:1 shape building model that complies with the AIJ guidelines [Mochida, 2002; Yuan, 2012]. The CFD setups and experimental data for verification can be found in the AIJ webpage (www.aij.or.jp/jpn/publish/cfdguide/index_e.htm). The inlet mean wind profile is the same as that given in the guidelines. The horizontal computational domain size is 172m × 108m. PALM does not allow differential grid spacing horizontally, an equidistant grid size of 1m is used. In the vertical direction, a grid size of 0.5m is adopted in below 24m and a stretch with a stretch factor of 1.05 is applied in above. With vertically 90 levels, the domain height is about 100m.

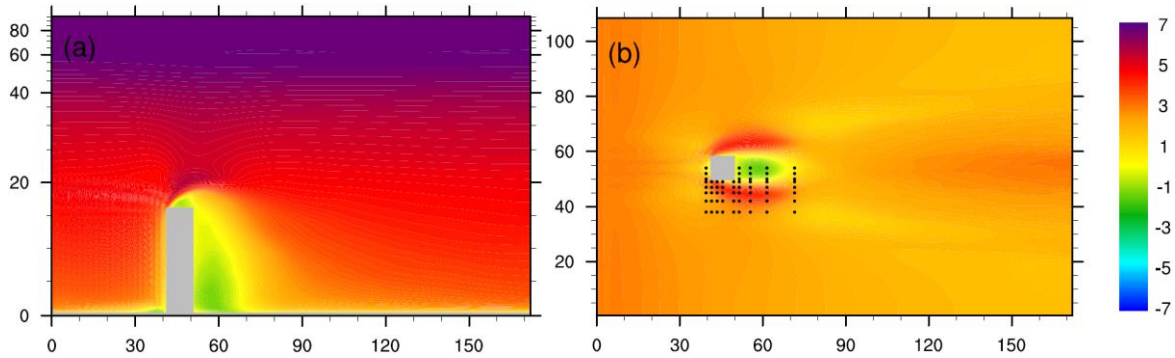


Figure 2: LES results of (a) vertical section of u-wind, and (b) horizontal section of u-wind at 1m height for validation of PALM codes. The grey box denotes the single building and black dots in (b) denote test-points for comparison in Figure 3b

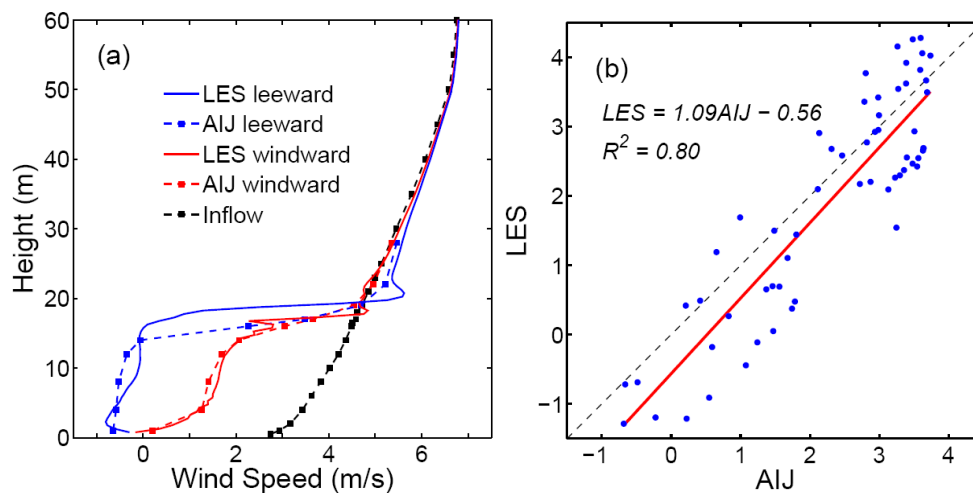


Figure 3: Cross-comparison between Architectural Institute of Japan (AIJ) experimental data and PALM results: (a) Vertical wind profiles in the windward (red lines) and leeward (blue lines) position at 2m from the building, the inlet mean wind is shown by the black profile. (b) Linear regression between AIJ and PALM results in the test points at 1m height shown in Figure 2b

The PALM-computed results for model validation are presented in Figure 2. Figure 2a is streamwise velocity of an x-z section located at the middle of the computational domain, while Figure 2b is streamwise velocity at 1m above ground. Correspondingly, Figure 3a compares velocity profiles at 2m away from the single building at windward (red lines) and leeward (blue lines), while Figure 3b is a scatter plot of PALM-computed and AIJ experimental velocity at 60 test points, which locations are shown in black dots of Figure 2b. Stronger rooftop vortex and velocity fluctuation compare to AIJ data can be observed from Figure 3a, but overall good agreement between the two suggests that PALM can capture the wind profile features around building. As this study focus on pedestrian-level ventilation, computational performance of PALM in reproducing near-surface velocity is more importantly. Cross-comparison of Figure 3b gives substantial confidence of using PALM in the present study.

4 Evaluation of ventilation over 3D building data

4.1 Effects of average size

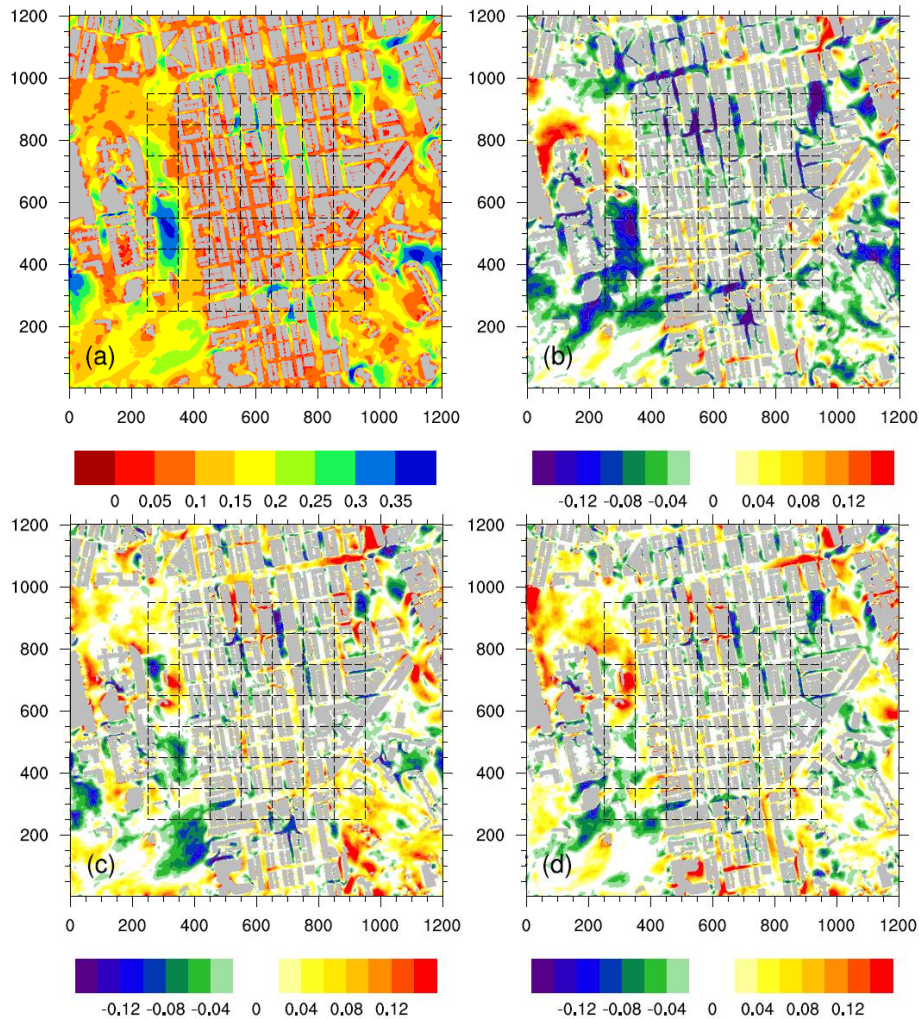


Figure 4: (a) PALM-computed VR in actual topography; deviations of VR from actual topography and topography retrieved from (b) Stereo images, (c) SAR images, and (d) fused result of the two images. The black dashed boxes denote the $100\text{m} \times 100\text{m}$ domains for zonally averaged VR. Wind input is from the east (right)

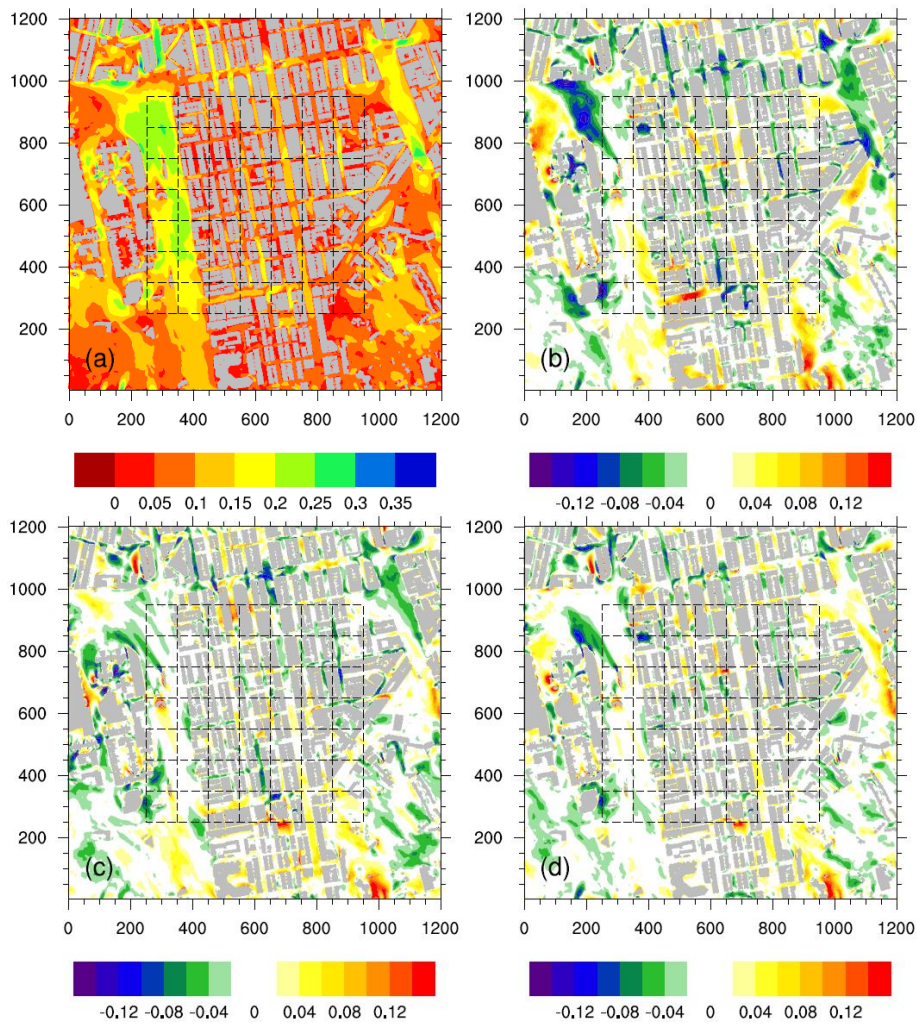


Figure 5: Same as Figure 4 but with wind input from the southwest

Wind direction	Average size	RMSEs Stereo	RMSEs SAR	RMSEs Fused
East	100m × 100m	0.040	<u>0.026</u>	0.028
East	50m × 50m	0.046	0.035	0.035
Southwest	100m × 100m	0.017	0.014	<u>0.009</u>
Southwest	50m × 50m	0.023	0.020	<u>0.016</u>

Table 1: Root mean square errors (RMSEs) of VR between extracted and actual building heights in different LES experiments (wind directions) and average sizes. The largest (smallest) value in each row is bolded (underlined)

Results of PALM-computed VR with wind input from the east (southwest) to actual topography and biases from extracted topography are given in Figure 4 (Figure 5). Urban planners and researchers may care more about the site-averaged VR than the VR at specific points. We select two kinds of grid sizes to check whether the comparative results are sensitive to this parameter. One is 100m × 100m while the other is 50m × 50m, with a unique buffer width of 250m. A buffer width of 250m can match the requirement of AVA [Ng, 2009], as the tallest building in the research area is 255m (Figure 1). Generally, it is suggested that

simulated results in the outer regions near the horizontal boundary are not reliable. The $100\text{m} \times 100\text{m}$ grids are shown in dashed boxes in Figures 4 and 5. For the grid size of $50\text{m} \times 50\text{m}$, the resolution is simply doubled.

Table 1 lists all the root mean square errors (RMSEs) of PALM-calculated VR between extracted and actual topography. The largest and smallest values in each row are highlighted, bolded for the largest value and underlined for the smallest value. Referring to the average size, the results can be compared for wind input from east and southwest respectively. It is found that the average sizes do not change the order of RMSEs from three sets of topography in case of southwest wind. The average size has a slight effect on the RMSE order in case of east wind, as can be seen from Table 2. Generally, the effects of average size on the overall RMSEs are not significant. Therefore, the scatter plots and linear regressions in Figure 6 are conducted with samples from the average size of $50\text{m} \times 50\text{m}$, which obtains more samples than an average size of $100\text{m} \times 100\text{m}$.

4.2 Effects of wind direction

Roughly speaking, VR is lower in the simulation with southwesterly input than in that with easterly input, which may be due to the street orientations in the area. Change in the input wind direction causes modifications in local (subdomains in the neighborhood) urban morphology and geometry parameters in AVA, such as the frontal area density. The local roughness length in the LES model takes effect when the wind sweeps across the ground and walls. The higher the proportion of ground and walls the wind has to sweep across, the larger the friction effects on the wind. Therefore, effects of wind direction on air ventilation are combined with local roughness length.

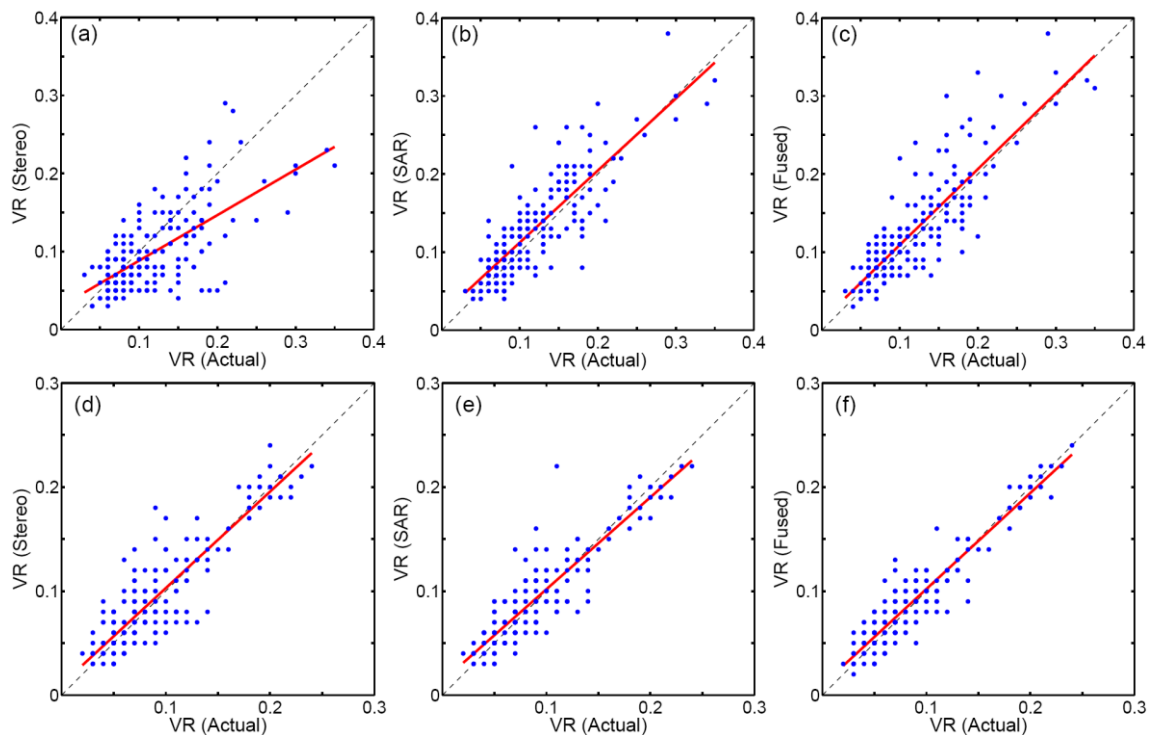


Figure 6: Scatter plots (blue dots) and linear regressions (red solid lines) of PALM-computed VR with actual topography and topography extracted from (a, d) Stereo image, (b, e) SAR image, and (c, f) fused result of the two images. Wind input is from the east (southwest) for a–c (d–f). Average size is $50\text{m} \times 50\text{m}$.

RMSEs in Table 1 suggest that building heights extracted from Stereo images give the worst performance compared with the other two methods. When comparing SAR and fused results, it is found that the fused results have better performance when given a southwest wind, while the SAR result is slightly better in case of east wind. Figure 6 further demonstrate the performance of data retrieved from different methods. It can be seen that the Stereo result has a large bias from the actual topography in the LES experiment with east wind (Figure 6a), while it has a better performance in the LES experiment with southwest wind (Figure 6d). The performances of SAR and the fused results are close to each other and reasonable in the LES experiment with both east and southwest wind (Figures 6b, c, e, and f).

4.3 Effects of building height

Using the average absolute difference from measured data to evaluate the retrieved results, Xu [2015] discovered that Stereo images provide better results for buildings below 100m, particularly for buildings below 50m, while SAR images provide better results for higher buildings (e.g., above 100 m). Tall buildings are underestimated by the Stereo images, which can be seen in Figure 1b. If we check the details of VR bias inside the congested urban spaces (dashed grid boxes in Figures 4 and 5), which are reliable because lateral boundary areas are avoided, it can be seen that a larger bias can be found in the Stereo result than in the SAR result in the simulations, particularly for wind input from the east. This implies that a better representation of higher buildings may contribute more to the quality of pedestrian-level ventilation simulations, as high-rise buildings can experience high wind loads and concentrate pedestrian-level winds [Liu, 2005; Yim, 2009].

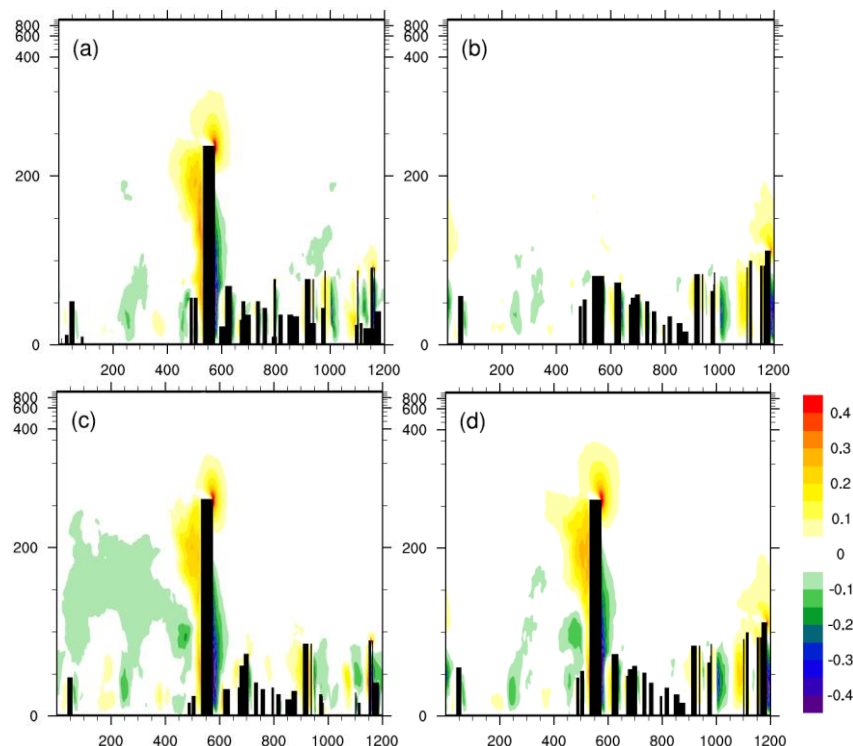


Figure 7: Time-averaged vertical velocity in a specific section with a high-rise building from (a) actual urban elevations, and urban elevations extracted from (b) Stereo image, (c) SAR image, and (d) fused result of the two images. The wind input is from the east (right)

We further demonstrate this dynamically using an extreme case: the tallest building is at a coordinate of approximately $x=550\text{m}$, $y=1000\text{m}$ (Figure 1). Figure 7 shows the vertical

velocity of the x-z cross section at $y=1000\text{m}$, which crosses the tallest building on the site. The results of the LES experiment with east wind input from all four topography datasets are shown. It is obvious that both the SAR and fused results can capture the high-rise building as well as the vertical motion around it, while the Stereo result fails to do so. When the wind comes from the east (right-hand side of Figure 7), the high-rise building blocks the wind and results in strong sinking motion on its windward side and rising motion in front of its steeple and on the leeward side. This vertical motion will further induce horizontal winds and gusts at the pedestrian level, and hence increase ventilation in the subdomain where the high-rise building stands. It is also noteworthy that a similar structure of vertical motion can be found around relatively high buildings in Figure 7, which suggests that better performance in representing higher buildings, rather than lower buildings, is more important in building height extraction for AVA purposes.

5 Discussion

Extraction of urban information from satellite images has become a hot topic in remote sensing studies [Colin-Koeniguer, 2014; Jin, 2005; Sportouche, 2011; Zhou, 2014], as these techniques are important for urban studies [Ren, 2011]. Therefore, assessment of these techniques should be done in combination with urban applications, which is the origin of the present study. As a case study, building information in a high-density urban area in Mong Kok, Hong Kong, including both actual information and that retrieved from satellite images, is adopted from a newly published report [Xu, 2015] and is evaluated by comparing pedestrian-level ventilation in an LES model. This is challenging because urban wind environments are extremely sensitive to urban morphologies and building geometries [Shi, 2015; Yang, 2013]. The accuracy requirement of urban geometries and building heights for AVA studies may be higher than that for other studies, such as thermal analysis without considering wind effects. As one can imagine, the effects of buildings on thermal conditions arise mainly through shading and anthropogenic heat generated by the buildings, and these effects are more localized than effects of building geometries on the wind environment.

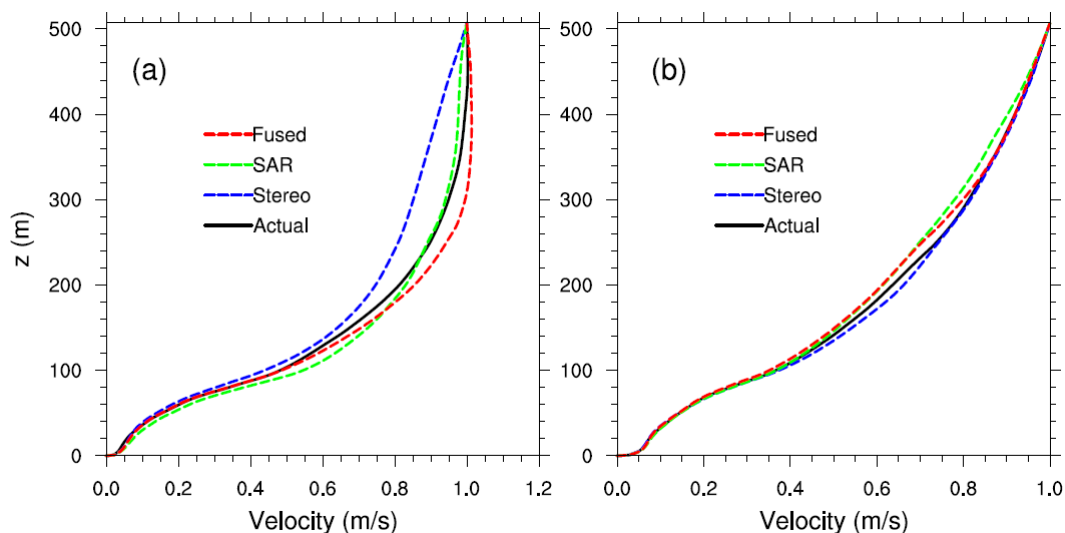


Figure 8: Horizontally averaged wind profile within the canopy normalized by the velocity at the canopy top (500m). (a) Wind input from the east, and (b) Wind input from the southwest

Our results show that simulated pedestrian-level wind speed is sensitive to the given wind directions, which in essence are sensitive to building geometries. The term “roughness length”

discussed in this study is not the city-scale roughness length that is applied in wind tunnel tests, but the so-called “local roughness length” that is imposed in each local grid box adjacent to a horizontal or vertical surface [Letzel, 2012]. The city-scale roughness length in front of the targeted area (a city or a neighbourhood) for generating the input wind profile in wind tunnel tests or CFD is not involved in the LES experiments in this study. The reason is to save simulation domain, and in turn, computational time. As mentioned, a vertically unique wind velocity is imposed. Associated with the cyclic boundary condition setting and adequate time (4 hours) for turbulence spin-up, a sufficient vertical wind profile can be generated in the simulation, as shown in Figure 8. Figure 8 also implies that the performance in reproducing the horizontally averaged velocity profile in the canopy layer is generally consistent with the performance in pedestrian-level VR. The result from Stereo data (dashed blue lines) has a larger discrepancy from the actual (solid black lines) compared to the SAR (dashed green line) and fused data (dashed red line), particularly for the case of wind input from the east (Figure 8a), which agrees with the scatter plot in Figure 6a showing the largest discrepancy when compared to other cases.

Finally, studies on urban wind environments using the LES technique require accurate urban morphologies and building geometries, i.e., precise urban elevation data. For the retrieved data used in this study, building footprints are assumed to be known before the building heights are extracted. Hence the street patterns are basically the same among all four sets of data evaluated in this study, and differences in pedestrian VR are caused mainly by building height and building volume differences. However, building footprints are probably not known, in the case of not knowing the realistic elevation data. Building height retrievals from satellite images without knowing building footprints and corresponding evaluations from the perspective of urban applications should be initiated in further studies.

6 Conclusions

This study performs a set of LES experiments using PALM to evaluate building height extraction from satellite images in an urban area of Mong Kok, Hong Kong. This comparative study is done from the practical perspective of urban ventilation. Major findings can be summarized as follows: First, building heights extracted from the Stereo image have the worst performance compared to those from the SAR image and the fused result of both images. Both the SAR and fused results can be considered acceptable for AVA purposes in this assessment in terms of their low RMSEs compared with the actual results. Second, it is known that high-rise buildings produce strong concentrated wind loads at the pedestrian level, and it is documented that data extracted from Stereo images produce better representations of low buildings, while data extracted from SAR images provide better results with high buildings. This may be the reason why a larger bias is found in the Stereo result than in the SAR result in both east and southwest wind simulations. A further implication for this point is that retrieval methods with better representation of higher buildings, and in turn better reproduction of the overall urban layer wind structure in CFD simulations, can obtain better urban ventilation results for AVA purposes.

Acknowledgments This study was supported by the Research Grants Council of the Hong Kong Special Administrative Region (Project No. 14408214), and Institute of Environment, Energy and Sustainability, CUHK (Project ID: 1907002).

References

- [Arnfield 2003] Arnfield A. J., Two decades urban research: a review of turbulence, exchanges of energy and water, and the urban heat island, *International Journal of Climatology*, vol. 23, Pages 1-26, 2003
- [Britter 2003] Britter R. E., Hanna S. R., Flow and dispersion in urban areas, *Annual Review of Fluid Mechanics*, vol. 35 no. 1, Pages 469-496, 2003
- [Castillo 2011] Castillo M. C., Inagaki A., Kanda M., The effects of inner- and outer-layer turbulence in a convective boundary layer on the near-neutral inertial sublayer over an urban-like surface, *Boundary-Layer Meteorology*, vol. 140 no. 3, Pages 453-469, 2011
- [Colin-Koeniguer 2014] Colin-Koeniguer E., Trouve N., Performance of building height estimation using high-resolution PolInSAR images, *IEEE Transactions on Geoscience and Remote Sensing*, vol. 52 no. 9, Pages 5870-5879, 2014
- [Eckert 2010] Eckert S., Hollands T., Comparison of automatic DSM generation modules by processing IKONOS stereo data of an urban area, *IEEE Journal of Selected Topics in Applied Earth Observation and Remote Sensing*, vol. 3 no.2, Pages 162-167, 2010
- [Emmanuel 2006] Emmanuel R., Johansson E., Influence of urban morphology and sea breeze on hot humid microclimate: the case of Colombo, Sri Lanka, *Climate Research*, vol. 30, Pages 189-200, 2006
- [Hong Kong Planning Department 2008] Hong Kong Planning Department, Working Paper 2B: Wind tunnel benchmarking studies, batch I, in: *Urban climatic map and standards for wind environment - feasibility study*, 587 pages, November 2008
- [Inagaki 2011] Inagaki A., Castillo M. C. L., Yamashita Y., Kanda M., Takimoto H., Large-eddy simulation of coherent flow structures within a cubical canopy, *Boundary-Layer Meteorology*, vol. 142 no.2, Pages 207-222, 2011
- [Jin 2005] Jin X., Davis C. H., Automated building extraction from high-resolution satellite imagery in urban areas using structural, contextural, and spectral information, *EURASIP Journal on Applied Signal Processing*, vol. 14, Pages 2196-2206, 2005
- [Kanda 2013] Kanda M., Inagaki A., Miyamoto T., Gryschka M., Raasch S., A new aerodynamic parameterization for real urban surfaces, *Boundary-Layer Meteorology*, vol. 148 no. 2, Pages 357-377, 2013
- [Keck] Keck M., Raasch S., Letzel M. O., Ng E., First results of high resolution large-eddy simulations of the atmospheric boundary layer, *Journal of Heat Island Institute International*, vol. 9 no. 2, Pages 39-43, 2014
- [Letzel 2008] Letzel M. O., Krane M., Raasch S., High resolution urban large-eddy simulation studies from street canyon to neighbourhood scale, *Atmospheric Environment*, vol. 42 no. 38, Pages 8770-8784, 2008
- [Letzel 2012] Letzel M. O., Helmke C., Ng E., An X., Lai A., Raasch S., LES case study on pedestrian level ventilation in two neighbourhoods in Hong Kong, *Meteorologische Zeitschrift*, vol. 21 no. 6, Pages 575-589, 2012
- [Lindberg 2010] Lindberg F., Grimmond C. S. B., Continuous sky view factor maps from high resolution urban digital elevation models, *Climate Research*, vol. 42 no. 3 Pages, 177-183, 2010

- [Liu 2005] Liu H., Jiang Y., Liang B., Zhu F., Zhang B., Sang J., Studies on wind environment around high buildings in urban areas, *Science in China Ser. D Earth Sciences*, vol. 48 Supp. 2 Pages, 102-115, 2005
- [Maronga 2015] Maronga B., Gryschka M., Heinze R., Hoffmann F., Kanani-Sühring F., Keck M., Ketelsen K., Letzel M. O., Sühring M., Raasch S., The Parallelized Large-Eddy Simulation Model (PALM) version 4.0 for atmospheric and oceanic flows: model formulation, recent developments, and future perspectives, *Geoscientific Model Development Discussions*, vol. 8 no. 2, Pages 1539-1637, 2015
- [Mochida 2002] Mochida A., Tominaga Y., Murakam S., Yoshie R., Ishihara T., Ooka R., Comparison of various κ - ϵ models and DSM applied to flow around a high-rise building — Report on AIJ cooperative project for CFD prediction of wind environment, *Wind Structure*, vol. 5, Pages 227-44, 2002
- [Ng 2009] Ng E., Policies and technical guidelines for urban planning of high-density cities – air ventilation assessment (AVA) of Hong Kong, *Building and Environment*, vol. 44 no. 7, Pages 1478-1488, 2009
- [Ng 2011] Ng E., Yuan C., Chen L., Ren C., Fung J. C. H., Improving the wind environment in high-density cities by understanding urban morphology and surface roughness: A study in Hong Kong, *Landscape and Urban Planning*, vol. 101 no. 1, Pages 59-74, 2011
- [Ng 2012] Ng E., Cheng V., Urban human thermal comfort in hot and humid Hong Kong, *Energy and Buildings*, vol. 55, Pages 51-65, 2012
- [Park 2012] Park S. B., Baik J. J., Raasch S., Letzel M. O., A large-eddy simulation study of thermal effects on turbulent flow and dispersion in and above a street canyon, *Journal of Applied Meteorology and Climatology*, vol. 51 no. 5, Pages 829-841, 2012
- [Park 2014] Park S. B., Baik J. J., Large-eddy simulations of convective boundary layers over flat and urbanlike surfaces, *Journal of the Atmospheric Sciences* 71(5):1880-1892, 2014
- [Raasch 2001] Raasch S., Schröter M., PALM - A large-eddy simulation model performing on massively parallel computers, *Meteorologische Zeitschrift*, vol. 10, Pages 363-372, 2001
- [Ramponi 2015] Ramponi R., Blocken B., de Coo L. B., Janssen W. D., CFD simulation of outdoor ventilation of generic urban configurations with different urban densities and equal and unequal street widths, *Building and Environment*, vol. 92, Pages 152-166, 2015
- [Razak 2013] Razak A. A., Hagishima A., Ikegaya N., Tanimoto J., Analysis of airflow over building arrays for assessment of urban wind environment, *Building and Environment*, vol. 59, Pages 56-65, 2013
- [Ren 2011] Ren C., Ng E., Katzschner L., Urban climatic map studies: a review, *International Journal of Climatology*, vol. 31 no. 15, Pages 2213-2233, 2011
- [Rodi 1997] Rodi W., Ferziger J. H., Breuer M., Pourquiée M., Status of large eddy simulation: results of a workshop, *Journal of Fluids Engineering*, vol. 119 no. 2, Pages 248-262, 1997
- [Schatzmann 2011] Schatzmann M., Leitl B., Issues with validation of urban flow and dispersion CFD models, *Journal of Wind Engineering and Industrial Aerodynamics*, vol. 99 no. 4, Pages 169-189, 2011
- [Shi 2015] Shi X., Zhu Y., Duan J., Shao R., Wang J., Assessment of pedestrian wind

environment in urban planning design, *Landscape and Urban Planning*, vol. 140, Pages 17-28, 2015

[Skote 2005] Skote M., Sandberg M., Westerberg U., Claesson L., Johansson A., Numerical and experimental studies of wind environment in an urban morphology, *Atmospheric Environment*, vol. 39 no. 33, Pages 6147-6158, 2005

[Sportouche 2011] Sportouche H., Tupin F., Denise L., Extraction and three-dimensional reconstruction of isolated buildings in urban scenes from high-resolution optical and SAR spaceborne images, *IEEE Transactions on Geoscience and Remote Sensing*, vol. 49 no.10, Pages 3932-3946, 2011

[Tamura 2008] Tamura T., Towards practical use of LES in wind engineering, *Journal of Wind Engineering and Industrial Aerodynamics*, vol. 96 no.10-11, Pages 1451-1471, 2008

[Tominaga 2008] Tominaga Y., Mochida A., Yoshie R., Kataoka H., Nozu T., Yoshikawa M., et al., AIJ guidelines for practical applications of CFD to pedestrian wind environment around buildings, *Journal of Wind Engineering and Industrial Aerodynamics*, vol. 96, Pages 1749-61, 2008

[Unger 2004] Unger J., Intra-urban relationship between surface geometry and urban heat island: review and new approach, *Climate Research*, vol. 27, Pages 253-264, 2004

[Wong 2011] Wong M. S., Nichol J., Ng E., A study of the “wall effect” caused by proliferation of high-rise buildings using GIS techniques, *Landscape and Urban Planning*, vol. 102 no. 4, Pages 245-253, 2011

[Xu 2015] Xu Y., Ma P., Ng E., Lin H., Fusion of WorldView-2 stereo and Multitemporal TerraSAR-X images for building height extraction in urban areas, *IEEE Geoscience and Remote Sensing Letters*, vol. 12, Pages 1795-1799, 2015

[Yang 2013] Yang F., Qian F., Lau S. S. Y., Urban form and density as indicators for summertime outdoor ventilation potential: A case study on high-rise housing in Shanghai, *Building and Environment*, vol. 70, Pages 122-137, 2013

[Yim 2009] Yim S. H. L., Fung J. C. H., Lau A. K. H., Kot S. C., Air ventilation impacts of the “wall effect” resulting from the alignment of high-rise buildings, *Atmospheric Environment*, vol. 43 no. 32, Pages 4982-4994, 2009

[Yuan 2012] Yuan C., Ng E., Building porosity for better urban ventilation in high-density cities – A computational parametric study, *Building and Environment*, vol. 50, Pages 176-89, 2012

[Zhou 2014] Zhou G. Q., Zhou X., Seamless fusion of LiDAR and aerial imagery for building extraction, *IEEE Transactions on Geoscience and Remote Sensing*, vol. 52 no. 11, Pages 7393-7407, 2014